

FOUR-DIMENSIONAL MARS CRATER RECONSTRUCTIONS USING 4-D SPLINE ALGORITHM

Maged Marghany

Geoinformation Global Space Technology
130B, Jalan Burhanuddin Helmi,
Taman Tun Dr. Ismail,
60000 Kuala Lumpur
Email:magedupm@hotmail.com

KEY WORDS: Mars, Crater, High Resolution Stereo Camera (HRSC), Four-dimensional, B-spline.

ABSTRACT: A crater is most visual characteristic which exists in Mars surface. Crater can be created through potential of two cosmic bodies crashed each other, for instance, a meteorite putting a planet. The foremost contribution of this work is to simulate 4-D of Mars craters. In doing so, 3-D information of HRSC used to be acquired and then 4-D spline algorithm carried out to sequences of HRSC archives with magnificent frame of times. The find out about suggests that B-spline can determine the 4-D go with the waft sample which ought to indicate for the existence of water. The sequence of elastic transforms for B-spline are used with involving computerized detection algorithm of landmarks. The examine about suggests that 4-D axis is seen certainly as floating objects on the center of crater. The study about additionally suggests that the deep of crater is blanketed thru ice which is an extraordinary proof of liquid water existence on the Mars. In conclusion, alternate of 4-D B-spline through involving elastic seriously change and landmarks algorithms ought to be a pinnacle notch promise for 4-D visualization.

1. INTRODUCTION

The dominant visible features which exist in Mars surface are the Craters. Crater may be created through two cosmic bodies crashed each different, as an instance, a meteorite putting a planet. It can be moreover long-established thru volcanic profession. The one of a kind form of crater is subsidence crater, which is occurred from an underground because of nuclear explosion. A crater-like pattern fashioned via erosion which is diagnosed as Machetes. Furthermore, a comfort crater triggered via a phreatic outburst or explosion is described as a maar crater. Therefore, Mars is a terrestrial planet which incorporates of minerals. These minerals are containing silicon and oxygen, metals, and exclusive factors which naturally structure rock. The Mars floor is ordinarily produced from tholeiitic basalt. With those regards, the Mars is needed elegant strategies to understand its complex nature and developments formation. In fact, man has an incredible hobby to find out Mars to be alternative agreement of the Earth. Presently, Marghany (2015a and 2015b) have pragmatic the fourth-dimensional set of rules to examine the geological crater factors of the Mars. Consequently, the initial geologic studies of Mars derived from floor-primarily based telescopic observations whilst the Mars and the Earth were neighboring and the spatial resolution was arisen as much as a hundred km decrease than the best earthbound atmospheric environment (Martin et al., 1992 and Rencz, 1999). Similarly, spacecraft orbiting Mars have brought images of canyons and flood valleys elements which endorse the life of water flows on the Mars floor. Nowadays, however, Mars is a cold, dry, wilderness like international thru a cracked ecosystem. Accordingly, no appeared organism must live on the purple Planet inside the absence of water flows (de Vaucouleurs, 1954; Mutch et al., 1976; Marghany and Mansor 2016).

Remote sensing applied sciences have attempted to discover the Mars surface. Spectroscopic far flung sensing observations for instance, can furnish widely investigative compositional and mineralogical statistics on the Mars surfaces. Basically, three classes of spectroscopic observations can be attained: (i) thermal emission spectra; (ii) reflectance spectra, and (iii) X-ray and gamma-ray spectra. Consequently, orbital seen and thermal-IR imaging and spectroscopic analyses by using the Mariner 9 and Viking missions displaying lavish supplementary geologically multifaceted floor which has been shaped by way of volcanic, tectonic, impact, and gradational processes. Credibly most discovery of dendritic valley network structures which were originated by the action of liquid water on the floor (Carr, 1996). Further, thermal-IR pix and near-IR imaging spectroscopic data, conveying evidence on the floor thermos-physical homes and mineralogy for inadequate region of the Martian floor (Rencz 1999; Hartmann, 2003). Moreover, X-ray and gamma ray are proficient to precisely extricate any object from its parent galaxy, and govern physical intensity in the nucleus, fingers and halo of spiral galaxy. Nonetheless, the shining objects that extract from

spiral galaxy for occasion with the aid of X-rays and gamma rays can be tiny and differ on timescales of few minutes or few seconds (Evans et al. 1993; Yin et al. 1993; Burns 1993; Gaffey et al. 1993).

Consistent with Marghany (2015a and 2015b), European Space Agency (ESA) has established the MARS specific mission which aimed at analyzing the surface, subsurface, environment and ionosphere of the Mars. The gadgets are expended for floor and subsurface research are implicated (i) High resolution Stereo Camera (HRSC); (ii) Visible and Infrared Mineralogical Mapping Spectrometer (OMEGA) and; Subsurface Sounding Radar Altimeter (MARSIS). Consequently, the atmosphere and Ionosphere gadgets are: (i) Energetic Neutral Atoms Analyzer (ASPERA); (ii) Planetary Fourier Spectrometer (PFS) and (iii) Ultraviolet and Infrared Atmospheric Spectrometer (SPICAM). Moreover, radio hyperlink instrument which is Mars Radio Science Experiment (MaRS). Conclusively, HRSC grants 3-D images of geological facets of the Mars which consists of surface, crust, and interior of the Mars. Certainly, the time period planetary geology science is to find out about the stable components of moons and planets.

Christensen, (1986) and Kahle et al., (1993) suggested that thermal emission spectra have been consumed, for instance, to acquire a proof on variations in continental basaltic lava flows and to confine rock abundance of the Martian surface and the thermal inertia. Moreover, Shelley (2008) referred to that the Hubble house Telescope (HST) is seemed the NASA's extraordinary dwelling observatories similarly to the Spitzer neighborhood Telescope, the Chandra X-ray and the Compton Gamma Ray space Observatories. Those vicinity observatories are designed to work with immoderate spectra electrical energy insurance which ranged from 20 keV to 30 GeV.

The novelty of this work is to layout algorithm for visualization of crater facets in four-dimensional the use of High resolution Stereo Camera (HRSC) images. In fact, HRSC can think about object in 3-D. With this regard, the foremost hypotheses is that 4-D of any object in area is coded into 3-d as 3D is coded into 2-D. On other words, $n+1$ D is coded into n -D. Through superior algorithm in computer vision, 4-D spline algorithm is believed to use in n -D visualization. With this regard, the study pursuits at utilizing 4-D spline to generate 4-D of crater surfaces from the stereo of craters which are acquired through High resolution Stereo Camera (HRSC).

2. DATA SETS

Figure 1 illustrates the physical design of HRSC. In fact, ESA's space probe Mars explicit was launched on June 2, 2003, through a Soyuz-Fregat rocket from Baikonur Cosmodrome in Kazakhstan. It entered the elliptical orbit of Mars on December 25, 2003. The orbit of Mars specific has a most distance of 10,530 km above the Martian floor and 330 km on adjoining approach. This physical geometry promises for examinations of the Mars moons Phobos and Deimos along with measuring its atmospheric profile (Marghany 2016).

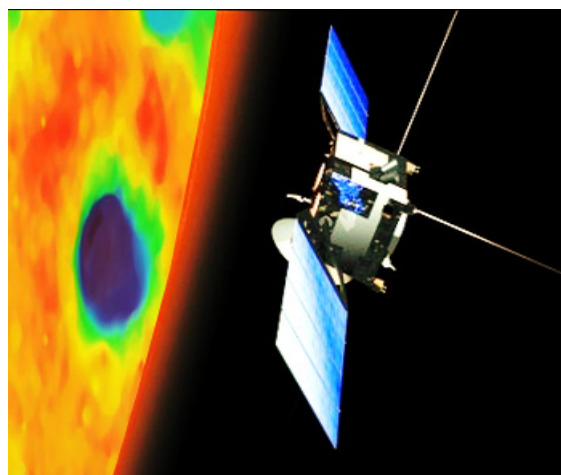


Figure 1. Mars Express in orbit around Mars.

Succeeding Marghany (2015a and 2015b), the crater data are acquired from HRSC. The HRSC is mapping the Mars in 3-D two with a resolution of about 10 meters (determine 2). Precise areas emerge as imaged at 2 m resolution. That is due to the digital camera encompasses extremely-excessive-decision telephoto lens barring awesome decision Channel (SRC), which is imaging objects to a few meters in size (DLR 2015). In preliminary

degree, the mission of HRSC is aimed closer to looking out liquid waters and existence inside the red Planet's surface. Thus far, about 75% of the Martian surface has been blanketed in 3-D.

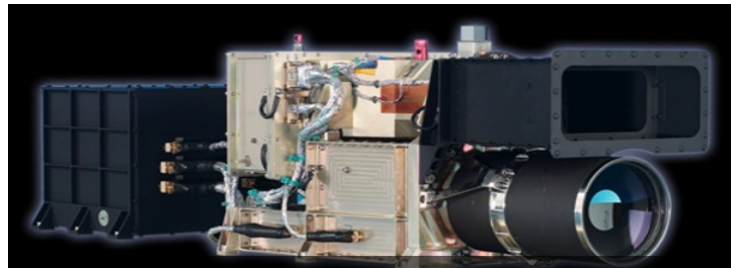


Figure 2. High Resolution Stereo Camera HRSC.

Figure 3 shows the HRSC camera scanning system. Consistent with Marghany and Mansor (2016) the HRSC camera system, which simplest weighs 20 kilograms, has two digital camera heads: the excessive resolution Stereo head, which consists of 9 CCD line sensors hooked up in parallel in the lower back of a lens. Approximately the shortest distance of 270 km from the spacecraft. Consequently, the resolution of the nine photo strips at this height is 12 m for each of the 5184 seven-micron rectangular pixels. The sensor has swath of 52 km and the minimal strip length of 300 km. The latter depends on the spacecraft's facts garage and transmission capability. The terrific resolution Channel (SRC) is used as a magnifying glass. On the epicenter, it grants pix of two. Three km wide inside the centre of the photo strips; the surface information are imaged with a decision of 2.3 m in step with pixel. The SRC recordings offer a geological background of the region, that's delivered by the high-decision imageries that are received with the stereo head (DLR 2015 and Marghany 2015s).

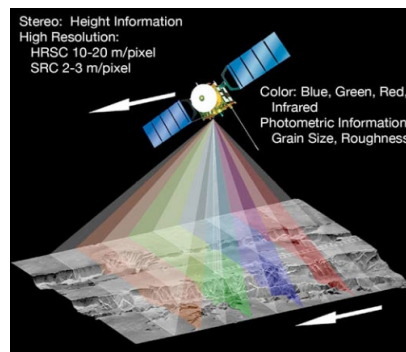


Figure 3. HRSC camera scanning system.

Further, the SRC head is composed of a reflect telephoto lens and a CCD array sensor. For instance, each sensor information the identical item at the surface at a one of a sort perspective. Three-dimensional images are generated with the aid of five of the image strips. The last 4 of the 9 line sensors are geared up with extraordinary coloration filters for recording multi-spectral facts (Marghany and Mansor 2016).

3. FOUR-DIMENSIONAL ALGORITHM

In physics and mathematics, the dimension of a mathematical space, is confidentially delineated for instance, the minimal range of coordinates required to become aware of any point contained by means of it. Space and time, in classical mechanics are various training and denote the supreme space and time. That conception of the objects is a four-dimensional (4-D) space, then again now not the one that was once originated integral to express electromagnetism. 4-D of space-time involve activities which are not sincerely termed spatially and temporally (Amini et al., 1998a; Marghany 2003; Marghany 2011; Marghany 2015b, Marghany and Mansor 2016). Otherwise, exceptionally are recognized as virtual to the motion of an observer. With these regards, any object can be power in the space of four and even higher dimensions. The key venture is to modify rationality tactics to renovate such high-dimensional stuffs. Following Marghany (2015b), 4-D spline is used to simulate 4-D of crater from sequences of HRSC images.

Assume u , v , and w are restrained to the interval two $u, v, w \in [0, 1]$ and $S(u, v, w, t) \in (x, y, z)$ (Amini et al., 1998b). This ability that the object is divided into hyperpatches. The hyperpatches are represented using surfaces and curves.

Then, the flooring described with the aid of inserting one of u , v , and w to a steady integer value which is yelled a knot plane which are the defining the surfaces of hyperpatches (Mortenson 1985). The factors in the in the interior and on the boundary of the parametric solid is assumed with the aid of Mortenson (1985),

$$p(u, v, w) = [x \ y \ z] = [x(u, v, w) \ y(u, v, w) \ z(u, v, w)] \quad (1.0)$$

Then, the constraints of equation 1 are given by

$$u_{\min} \leq u \leq u_{\max}; \quad (2.0)$$

$$v_{\min} \leq v \leq v_{\max}; \quad (3.0)$$

$$w_{\min} \leq w \leq w_{\max} \quad (4.0)$$

The 4-D B-spline curve is well-defined by means of the subsequent equation ($n_k = n$):

$$C(t) = \mathbf{N}_{n \times 3} \cdot \mathbf{P}_{n \times 3} = \begin{pmatrix} N_{0,p}(t) & N_{1,p}(t) & \dots & N_{n-1,p}(t) \end{pmatrix} \begin{pmatrix} P_{0,x} & P_{0,y} & P_{0,z} & P_{0,t} \\ P_{1,x} & P_{1,y} & P_{1,z} & P_{1,t} \\ \dots & \dots & \dots & \dots \\ P_{n-1,x} & P_{n-1,y} & P_{n-1,z} & P_{n-1,t} \end{pmatrix}, \quad (5.0)$$

where $N_{i,p}(t)$ – B-spline basis competencies and a manage factor matrix is $\mathbf{P}_{n \times 3}$. To enforce the 4-D spline, the 3-D HRSC data that is assimilated at specific knot time and knot planes turn out to be temporal features. Then the detected facets in 3D HRSC can be expressed in four-D B-spline model as (Amini et al., 1998a):

$$R(u, v, w, t) = \sum_{i=1}^I \sum_{j=1}^J \sum_{k=1}^K \sum_{l=1}^L P_{ijk} O_i(u) O_j(v) O_k(w) O_l(t) \quad (6.0)$$

where $O_i(u)$, $O_j(v)$, $O_k(w)$, and $O_l(t)$ are B-spline basis functions which blend control points $\mathbf{P}_{n \times 3}$ and $(I \times J \times K \times L)$ is the total number of model control points. By changing the order of B-spline summation, a more efficient approach to computing a multi-dimensional B-spline model results. The simulated data included 300 frames. The fitting algorithm converged in about 30 iterations. Therefore, the total fitting process approximately took 588 seconds for 6 frames of data. An important byproduct of our approach is that at the conclusion of fitting knot solid to frames of data, a 4-D model $S(u, v, w, \text{and } t)$ is determined. Given two solids $S(u, v, w, t_0)$ and $S(u, v, w, t_1)$, a 3-D B-spline interpolated motion field is immediately generated by employing the computation in (Amini et al., 1998b):

$$V(u, v, w) = S_1(u, v, w, t_1) - S_0(u, v, w, t_0) \quad (7.0)$$

The 4-D shape mannequin is self-regulating of the intrinsic description of 3-D and 4-D figures when landmarks are existing. It can be effortlessly prolonged to 4-D case after normalizing the variety of phases per exclusive sub-images of all frames to subjective range of data. In this learn about we used 30 frames, and using the landmark advent algorithm continually for each section of 30 frames over time t . Then, a collection of elastic transforms are implemented to bring the transmitted landmarks on pinnacle of the crater surface. The following equation is used for a series of elastic transforms as

$$\mathbf{T}_{elastic}(u, v, w, t) = [u, v, w, t]^T + \sum_{i=1}^I \sum_{j=1}^J \sum_{k=1}^K \sum_{l=1}^L P_{ijk} O_i(u) O_j(v) O_k(w) O_l(t) M_{i+l, j+m, k+n, L+o} \quad (8.0)$$

where M denotes $N_u \times N_v \times N_w \times N_t$ mesh for control point of $[u, v, w, t]^T$ which are identified within a volume of dimension of $[U, V, W, t]$. The elastic transforms were achieved with a series of B-spline changes by four levels of meshes, $(4 \times 4 \times 4)$, $(6 \times 6 \times 6)$, $(8 \times 8 \times 8)$, and $(16 \times 16 \times 16)$. Its allied control points for each mesh level, M are adjusted to minimize the space between the distorted landmarks and the number of object surface.

4. RESULTS AND DISCUSSION

Evidently, the craters DEM inside the Hellas Basin is exposed in Figure 4. It is thrilling to find that the DEM varies between -3 km to 6 km. Craters geographical location is 29°S , and 68°E in northern rim of Hellas basin. This archives data acquired on 8 July 2004 by way of HRSC digital camera. Corresponding to Marghany (2015a), the Hellas Basins have formed among between 3.8 and 4.1 billion years in the past, after a terrific asteroid hit the Mars surface. These

Hellas basins have been modified by the possessions of wind motion, ice, water and volcanic hobby for the reason that they had been shaped. As well, HRSC become able to imagine the craters with the ground resolution is about 15 m in line with pixel with 25 km across. Figure 5, indicates the simulated crater DEM which ranged from -3km to 3km. The bottom point of DEM of -3km is located in deep of the crater.

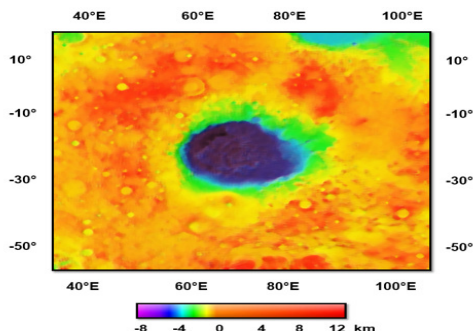


Figure 4. Craters DEM Hellas Basin.

The bulky of the two craters is about 25 km across. Therefore, the morphology of many facets in the Hellas Basin and its environment strongly suggests the presence of ice and glaciers. The HRSC can produced 3-D of Mars geological facets due to the fact of the High Resolution Stereo head works on push broom mode: sensors photo a line on the planet floor perpendicular to the ground track of the spacecraft and matter on the orbital movement of the spacecraft to reposition them as they greatest a sequence of photos recognized as an image swath. This agrees with the studies of Hartmann (2003); Carr (2006); and Marghany (2015a and 2015b).

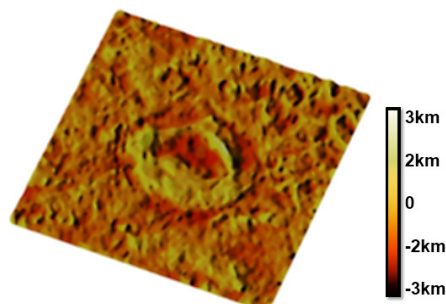


Figure 5. 3-D of crater simulated by B-spline.

Figure 6 suggests the 4-D of the crater which simulated using 4-D spline. It is fascinating to locate that 4-D layer is considered truly as floating on the center of crater. In addition, the deep of crater is dominated through ice which is the proof of liquid water existence. This should attribute to that inside -3km in deep of crater, the atmospheric stress is about 89% greater than the surrounding of the crater. This discovering consents with Marghany (2015a) and ESA (2015). Truthfully, 4-D spline algorithm is separated 3-D craters from HRSC data into hyperpatches. Subsequently, the hyperpatches are carried out the use of surfaces and curves. Formerly, the floor labeled by way of tracing one of 3-D elements to a consistent integer price which are the major of hyperpatches.

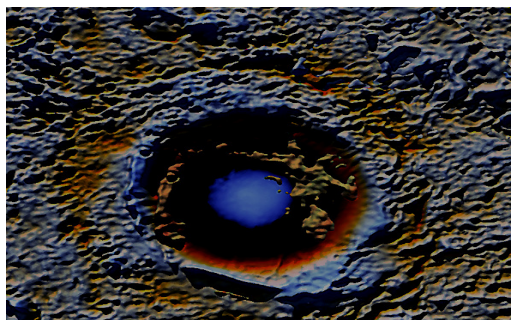


Figure 6. 4-D crater simulated by B-spline.

4-D is engendered robotically through aid of innovations. Indeed, innovations are routinely created and transmitted to

4-D information with the aid of skill of rigid alignment, distance-based merging, and B-spline transform. The energy of series of elastic transforms which are recognized inside an extent of 4-D dimension. This is simply obvious in Figure 6. Additionally, the sequence of B-spline changes are carried out through the elastic transforms to gather precisely 4-D of crater volumetric. The landmarks are compulsory to be constantly scattered on the crater surface and concentrated ample consequently that their triangular mesh is adjoining to the original crater surface. Predominantly, landmarks positioned on crater surfaces have to fit up to every pixel. Finally, M are adjusted to minimize the firm between the distorted landmarks and the wide variety of object surface. This learn about confirms the work completed by way of Waks et al., (1996); Duda, (2001); Marghany (2014); and Marghany (2015b); Marghany and Mansor (2016).

5. CONCLUSIONS

This finds out about has verified a brand new novelty for four-D crater floor reconstruction of HRSC information. The sequence of elastic transforms for B-spline are used with regarding the automatic detection algorithm of landmarks. The seem at suggests that 4-D axis is seen definitely as floating devices at the core of the crater. The find out about additionally suggests that the deep of the crater is included through potential of ice that is a magnificent evidence of liquid water lifestyles at the Mars. It can be said that exchange of 4-D B-spline through way of regarding elastic redecorate and landmarks algorithms may want to be a pinnacle notch promise for 4-D visualization.

References

- Amini, A.A., Y. Chen, R. W. Curwen, V. Mani, and J. Sun, 1998a, Coupled B-Spline Grids and Constrained Thin-Plate Splines for Analysis of 2-D Tissue Deformations from Tagged MRI", *IEEE Transactions on Medical Imaging*, 17(3):344-356.
- Amini, A.A., P. Radeva, and D. Li, 1998b, Measurement of 3D motion of myocardial material points from explicit B-surface reconstruction of tagged data", *Medical Image Computing and Computer-Assisted Intervention*, MIT, Cambridge, MA, October 1998.
- Burns R.G., 1993. Origin of Electronic Spectra of Minerals in the Visible-Near Infrared Region. In *Remote Geochemical Analysis: Elemental and Mineralogical Composition*, ed. C.M. Pieters and P.A.J. Englert, pp. 3-29. Cambridge: Cambridge Univ. Press.
- Carr, M 2006. *The surface of Mars*. Cambridge, UK: Cambridge University Press.
- de Vaucouleurs G., 1954. *Physics of the Planet Mars*. Faber and Faber, London.
- Duda, R. O. , Hart, P. E. and Stork, D. G. 2001. *Pattern Classification*. John Wiley & Sons, Inc.
- ESA 2015, Craters within the Hellas Basin. http://www.esa.int/spaceinimages/Images/2014/08/Craters_within_the_Hellas_Basin. [Access on August 20 2015].
- Christensen, P.R., 1986. The spatial distribution of rocks on Mars, *Icarus*, 68, 217-238.
- Evans, L.G., R.C. Reedy, and J.I. Trombka, (1993). Introduction to planetary remote sensing gamma ray spectroscopy, in *Remote Geochemical Analysis: Elemental and Mineralogical Composition*, C.M. Pieters and P.A.J. Englert, eds., Cambridge Univ. Press, pp. 167-198.
- Gaffey S.J., L.A. McFadden, and D.B. Nash, 1993. Ultraviolet, visible, and near-infrared reflectance spectroscopy: Laboratory spectra of geologic materials. In *Remote Geochemical Analysis: Elemental and Mineralogical Composition*, C.M. Pieters and P.A.J. Englert, eds., pp. 43-71. Cambridge: Cambridge Univ. Press.
- Hartmann, W. (2003). *A Traveler's Guide to Mars: The Mysterious Landscapes of the Red Planet*. New York: Workman Publishing.
- Kahle, A.B., F.D. Palluconi, and P.R. Christensen, 1993. Thermal emission spectroscopy: Application to the Earth and Mars, in *Remote Geochemical Analysis: Elemental and Mineralogical Composition*. C.M. Pieters and P.A.J. Englert, eds., Cambridge Univ. Press, pp. 99-120.

- Marghany, M., 2003, July. Polarised AIRSAR along track interferometry for shoreline change modeling. In *Geoscience and Remote Sensing Symposium, 2003. IGARSS'03. Proceedings. 2003 IEEE International* (Vol. 2, pp. 945-947). IEEE.
- Marghany, M., 2011. Modelling shoreline rate of changes using holographic interferometry. *International Journal of Physical Sciences*, 6(34), pp.7694-7698.
- Marghany M., 2014. Hologram interferometric SAR and optical data for fourth-dimensional urban slum reconstruction. Proceedings of 35 th Asian conference on remote sensing, Nay Pyi Taw, Myanmar from 27- 31, October 2014. <http://a-a-r-s.org/acrs/administrator/components/com.../OS-303%20.pdf>. [Access on August 20 2015].
- Marghany M., 2015a. 4-D geological feature reconstructions in Mars using High Resolution Stereo Camera (HRSC). CD of 36th Asian Conference on Remote Sensing (ACRS 2015), Manila, Philippines, 24-28 October 2015, http://www.a-a-r-s.org/acrs/administrator/components/com_jresearch/files/publications/TH2-5-5.pdf.
- Marghany M., 2015b. Fourth-dimensional optical hologram interferometry of rapid eye for Japan Tsunami effects. 36th Asian Conference on Remote Sensing: Fostering Resilient Growth in Asia, ACRS 2015; Crowne Plaza Manila Galleria Quezon City, Metro Manila; Philippines; 24 October 2015 - 28 October 2015.
- Marghany M., and Mansor S., 2016. Four-dimensional B-spline Algorithm for MARs Crater Reconstructions. CD of 37th Asian Conference on Remote Sensing (ACRS), 37th ACRS from 17th - 21st October 2016, Galadari Hotel, Colombo, Sri Lanka, pp.1-6. www.a-a-r-s.org/acrs/administrator/components/com_jresearch/.../Ab%200641.pdf
- Martin, L.J., P.B. James, A. Dollfus, K. Iwasaki, and J.D. Beish, 1992. Telescopic observations: Visual, photographic, polarimetric, in *Mars*, edited by H.H. Kieffer, B.M. Jakosky, and M.S. Matthews, pp. 34-70, Univ. of Ariz. Press, Tucson.
- Mortenson, M.E. 1985, *Geometric Modeling*. John Wiley & sons, New York.
- Mutch, T.A., R.E. Arvidson, J.W. Head III, K.L. Jones, and R.S. Saunders, 1976. *The Geology of Mars*, Princeton Univ. Press, Princeton NJ.
- Radeva, P., Amini, A., Huang, J. 1997. Deformable B-solids and implicit snakes for 3D Localization and tracking of SPAMM MRI Data. *Computer Vision and Image Understanding* 66, 163–178.
- Rencz, A. N. 1999. *Remote sensing for the earth sciences: manual of remote sensing Volume 3* (No. Ed. 3). John Wiley and sons.
- Sheehan, W., 1988. *Planets and Perception*, Univ. Arizona Press.
- Shelley C., (2008) NASA's Great Observatories. NASA. Retrieved April 26, 2008
- Waks, E., Prince, J., Douglas, a 1996. Cardiac Motion Simulator for Tagged MRI. *Mathematical Methods in Biomedical Image Analysis*, 182–191.
- Yin, L.I., J.I. Trombka, I. Adler, and M. Bielefeld, 1993. X-ray remote sensing techniques for geochemical analysis of planetary surfaces, in *Remote Geochemical Analysis: Elemental and Mineralogical Composition*, C.M. Pieters and P.A.J. Englert, eds., Cambridge Univ. Press, pp., 199-212.